Versatile semi-batch apparatus for manometric measurement of gas-solid reaction rates

Heidlage, Michael Gregory
Aloi, Michael J.
Nobile, Arthur Jr.
Safarik, Douglas Joseph

To be published in: Review of Scientific Instruments

DOI to publisher's version: 10.1063/5.0058181

Versatile Semi-Batch Apparatus for Manometric Measurement of Gas-Solid Reaction Rates

Michael G. Heidlage,[1] M. J. Aloi,[1] and D. J. Safarik[1]*

[1]Sigma Division, Los Alamos National Laboratory, Los Alamos, NM 87544, U.S.A.

*Corresponding author e-mail: dsafarik@lanl.gov

Abstract

We describe the design, construction, operation, and performance of a simple and versatile semi-batch reactor that is especially useful for measurement of gas/solid reaction rates at pressures in the range of 1 mtorr to 1500 torr. The reactor operates by repeatedly imposing small AC modulations of reactant gas pressure on top of a much larger DC pressure background. Based on the rate of pressure relaxation following each AC pulse, the reaction rate is determined. Our design is characterized by modular construction from off-the-shelf, ultra-high-vacuum-compatible components, which facilitate easy retrofitting and adaptation to a range of experimental conditions. Automated experiment control and data acquisition is accomplished via a custom National Instruments© LabView virtual instrument. Data analysis is automated using a custom series of Mathworks© Matlab scripts. We demonstrate reactor performance through measurements of hydrogenation kinetics for a composite H_2 getter material consisting of 1,4-bis(phenylethynyl)benzene mixed with a palladium/carbon catalyst.

I. Introduction

The purpose of measuring reaction rate kinetics is to parameterize the chemical process rate in terms of conversion, temperature, and reactant and product concentrations (pressures).[1] From a scientific perspective, this parameterization is crucial to the investigation of kinetic networks and reaction mechanisms, and to the establishment of rate-limiting step(s).[2-4] From an engineering perspective, kinetic measurements can guide manufacturing process development, and facilitate accurate and quantifiable predictions regarding process behavior. Of course, these goals are not mutually exclusive; scientific insight can lead to clever engineering solutions, for example industrial use of contact membrane reactors to overcome low hydrogen solubility in three-phase heterogeneous catalytic hydrogenation processes.[5, 6]

In the study of gas-solid chemical reactions, gravimetric-based methods are commonly used to measure reaction kinetics. This is primarily due to the ubiquity of commercial instrumentation, relatively simple implementation, and applicability to many chemical systems.[1, 7-10] Of course, for gravimetric methods to be effective, the mass of the solid must change. However, not all gas-solid reactions are well-suited to study by gravimetric methods. Indeed, any change in the solid mass that does not directly correlate with the kinetic process of interest can convolute interpretation of the rate data. For example, when the process of interest is an addition-type reaction,

$$A_{(s)} + B_{(g)} \rightarrow C_{(s)} \tag{1}$$

any process that carries away solid mass, for example sublimation of the solid or the evolution of incidental gaseous products such as CO_2, H_2O, or light hydrocarbons, will likely complicate the kinetic analysis.

In our laboratory, we are particularly interested in the reaction of hydrogen gas with solid unsaturated organics such as 1,4-bis(phenylethynyl)benzene (DEB), shown in Fig. 1. When combined with a H_2 dissociation catalyst, DEB and similar unsaturated organics, for example 1,2-diphenoxy-2,4-hexadiyne (DPPE)[11, 12] and 1,4-diphenylbutadiyne (DPB),[13-15] function as hydrogen getters that scavenge H_2 and prevent it from accumulating in sealed containers. This scavenging can mitigate a potential explosion hazard or hydrogen corrosion of materials.[16-18] In the presence of a Pd catalyst supported on activated carbon (Pd/C), DEB reacts irreversibly with H_2 ($\Delta G_{Rxn} \approx$ -600 kJ/mol DEB, estimated from the enthalpy of acetylene hydrogenation)[19] via a complex mechanism that results in several products or intermediates,[20] some of which are orders of magnitude more volatile than the DEB reactant itself.[21, 22] For a range of reaction conditions of interest to us, the mass lost due to volatility is comparable to mass gained due to incorporation of H or D atoms into the DEB molecular structure (~3%).[21] As such, we were forced to consider alternatives to gravimetric techniques to measure meaningful kinetic data.

Manometric methods have been used for decades to measure reaction kinetics.[23-25] Of particular note is the Sieverts' technique, which is commonly used to quantify gas-solid phase equilibria. Although often referenced in the context of H_2/metal systems,[26-32] the Sieverts' method is broadly applicable to quantification of gas sorption for most gas/solid systems, and serves as the underlying principle in many commercially available physisorption and chemisorption instruments.[33-36] Detailed descriptions of the process, instrument design, and operational considerations can be found in the literature.[35, 37-39]

Although the Sieverts' apparatus is best-suited to thermodynamic measurements of gas-solid equilibria, it is often used to investigate and even quantify hydrogen sorption and desorption rates in H_2/metal systems.[6, 40-43] The Sieverts' method is less than optimal for accurate measurement of reaction rates, mainly because during equilibration of each gas aliquot the pressure often decreases by a large fraction of its initial value. A large pressure drop is ubiquitous for reactions that are essentially irreversible ($\Delta G_{Rxn} << 0$), such as reaction of H_2 with DEB getters. In this case, the equilibrium H_2 gas pressure is effectively zero, and the pressure decrease is equal to the initial aliquot pressure.

Because the reaction rate usually depends on pressure (e.g., first- or second-order kinetics), a large pressure drop results in a non-linear pressure decay trace whose kinetic analysis often requires either differentiation or fitting with an assumed rate law. The first approach can potentially result in excessively noisy rate data, whereas the second may bias the analysis and interpretation of the data. We should point out, however, that the thermal analysis community has enjoyed significant success in remedying excess noise in differentiated signals via polynomial data fitting, data smoothing and filtering techniques, as well as improved experimental methods such as using a proper sampling rate.[1, 10] Furthermore, model-free kinetic analyses such as isoconversional methods have been increasingly used to avoid the hazards associated with incorrect model fits.[44] As discussed in the following sections, our goal by directly measuring the reaction rate instead of the conversion (accumulated signal) is to avoid these methods by rendering them unnecessary.

To accurately quantify the kinetics of gas/solid reactions, whether irreversible such as H_2/DEB, or reversible with finite equilibrium pressures such as many H_2/metal systems, we have developed a semi-batch, automated, manometric-based reactor system. This system *directly* measures the reaction rate in real time at isothermal and practically isobaric conditions. It is constructed from commercially available, off-the-shelf, ultra-high-vacuum hardware and is controlled using custom software that we have written using National Instruments© (NI) LabView.[45] Furthermore, we have developed computer code in Mathworks© Matlab that automates analysis of the acquired data, thereby significantly reducing data processing time.[46] In this paper we apply this measurement system to the catalytic hydrogenation of DEB while providing a detailed description of the apparatus design and construction, experimental procedures, and automated analysis methods. Our experience and results suggest that the reactor design is likely applicable to a wide assortment of gas/solid chemical systems.

II. Instrument Design, Operation, and Control

Description of Apparatus. A schematic of our apparatus is shown in Fig. 2. The main reactor vessel, shown with DEB-Pd/C pellets inside (Honeywell National Security Complex, 75% DEB, 1.25% Pd, 23.75% activated carbon by weight), is a "spherical octagon" ultra-high vacuum chamber available commercially from Kimball Physics (No. MCF600-SphOct-F2C8). We have modified this chamber by gold-plating the walls to mitigate sorption/desorption of hydrogen by the stainless steel. Helium and N_2 purge/diluent gases are delivered directly to the reactor without further purification via manually controlled, ultra-high-vacuum precision leak valves (MDC Vacuum Products, LLC No. 315010). Research-grade H_2/D_2 reactant gas undergoes additional purification using a Pd-Ag membrane purifier (REB Research and Consulting, Mr. Hydrogen), and is then delivered to the reactor through a piezo-electrically controlled, ultra-high vacuum doser/leak valve (Oxford Applied Research, Ltd., No. PLV-1000). All gases are supplied from pressurized cylinders (Airgas, Inc.).

In addition to the main reactor vessel, the system also contains a gold-plated reference vessel, labeled (h) in Fig. 2, which is essentially identical to the main reactor and connected to it through metal-seal valves. As discussed later, the reference vessel is used when the H_2/D_2 reaction rate is measured in the presence of an inert background gas.

Pressures in the main reactor and reference vessel are measured using 1 and 1000 torr high-accuracy absolute capacitance manometers (MKS Instruments, Inc. Baratron® Nos. 120AA-00001RCJ and 120AA-01000RCJ, respectively). In the case where an inert background gas is used, the pressure *difference* between the reactor and reference vessels is measured using a 1 torr high-accuracy differential pressure manometer (MKS Instruments, Inc., Baratron® No. 120AD-00001RCU). These manometers can easily be changed to ones of other pressure ranges-we also commonly use 0.1 torr high-accuracy Baratron® manometers (not shown in Fig. 2). We should note that experiments at pressures up to ~1500 torr absolute are possible in these reactors. This upper limit is dictated by the UHV, conflat-flanged hardware.

The system is evacuated by a pumping station that contains a turbomolecular pump backed by a diaphragm pump (Pfeiffer Vacuum, Inc., HiCube 80 Classic No. PM-S22-240-00, HiPace80 turbopump, and MVP 070 diaphragm pump). A quadrupole mass spectrometer (Pfeiffer Vacuum, Inc., Prisma Plus, No. QME 220) is used to qualitatively analyze the gas phase.

All tubulation in the system is ½ or ¼ in. diameter solid electropolished stainless or flexible stainless (Swagelok, CT Series), and all fittings are either Conflat® or VCR® (Swagelok). With the exception of the ultra-high-vacuum leak valves and the gate valve at the pump (see Fig. 2), valves are all-metal and bellows-sealed (Swagelok, SS-4H-VCR and SS-4H-V51).

Most of the reactor system is contained within a Friocell laboratory incubator (BMT Medical Technology, No. FC-B2V-M/FC111) that controls temperature in the range 0-100 ± 0.05°C. The extent of the Friocell envelope is illustrated in Fig. 2. Control of the H_2/D_2 gas pressure (via operation of the piezoelectric leak/doser valve) and acquisition of pressure and temperature data are accomplished using National Instruments© LabView software installed on a Windows 10 PC.

Description of Operation, with Application to DEB Getter Hydrogenation. Figure 3 shows typical pressure and mols H_2 vs. time data for the reaction of pure H_2 gas with DEB-Pd/C getter pellets in our semi-batch reactors. We will now discuss in detail the measurement of reaction rates with reference to Fig. 3. Similar to most manometric measurements, we start by injecting

H_2 gas into the reactor. For the experiment shown in Fig. 3, we inject neat H_2, without a background gas, until a total pressure of 765 mtorr is achieved. We consider this to be the sum of a nominal mean pressure (P_{Mean} = 750 mtorr in Fig. 3, panels (a) and (b)) plus ½ of a pulse pressure (½ΔP_{Pulse} = 15 mtorr). The dosing is done using the computer-controlled, PLV-1000 piezoelectric doser/leak valve. After dosing, we measure the time dependence of the subsequent pressure relaxation due to the (irreversible) reaction of H_2 with the DEB-Pd/C. We allow the pressure to decay by ΔP_{Pulse}, from P_{Mean} + ½ΔP_{Pulse} = 765 mtorr to P_{Mean} – ½ΔP_{Pulse} = 735 mtorr. In a typical experiment for DEB hydrogen getters, we use $\Delta P_{Pulse}/P_{Mean} \approx 4\%$ to maintain near-linearity of the pressure relaxation. Once a pressure of P_{Mean} – ½ΔP_{Pulse} = 735 mtorr is achieved, additional gas is dosed into the reactor, boosting the pressure by ΔP_{Pulse} to P_{Mean} + ½ΔP_{Pulse} = 765 mtorr. As shown in Fig. 3, panels (a) and (b), this pressure pulse and decay cycle is repeated until the desired conversion is achieved, or until the reaction rate becomes impractically slow to measure. The result is a reproducible sawtooth waveform with average pressure P_{Mean} and peak amplitude ½ΔP_{Pulse}. In this way, our experiment probes the reaction rate by repeatedly superimposing a small AC pressure modulation of ±½ΔP_{Pulse} on top of a constant DC pressure of P_{Mean}.

Note that this approach contrasts with the Sieverts'-type method, wherein after each gas injection the pressure is allowed to decay until equilibrium is achieved (in the case of reversible reactions), until the gas is completely consumed (in the case of irreversible reactions), or until the solid is fully reacted. Often, the relative pressure decrease associated with Sieverts' experiments is large, up to 100% of the initial pressure injection. As discussed below, this has negative consequences for accurate determination of the reaction rate.

Figure 3(c) shows the time dependence of the mols of H_2 in the gas phase, calculated using the pressure vs. time data in Fig. 3(b), the measured reactor temperature and volume, and the ideal gas law. In Fig. 3(c) we denote the local maxima and minima in mols of H_2 gas using black squares and circles, respectively. In general, the pressure relaxation will be nonlinear *except* in the case of a gas-solid reaction that is zeroth-order in the reactant gas pressure, i.e., P_{H2}^n where n = 0. However, for an arbitrary reaction order n, a sufficiently small magnitude of the pressure pulse will result in a relaxation that is *virtually* linear. The reason is that for a small pulse, P_{Mean} + ½ΔP_{Pulse} and P_{Mean} - ½ΔP_{Pulse} are sufficiently similar that the rate $R \propto P_{H2}^n$ is functionally the same at the two pressures. Viewed differently, when the magnitude of the pressure relaxation is small, so too is the incremental increase in conversion. Over this small increment of conversion, the reaction rate is essentially constant and thus the pressure relaxation is, for practical purposes, linear. Although it is difficult to generalize considering the wide array of gas-solid reactions, we believe that this reasoning applies to any reaction whose rate is a continuous and well-behaved function of conversion.

The above discussion explains our rationale for using a small AC pressure modulation relative to the DC pressure in our experiments ($\Delta P_{Pulse}/P_{Mean} \approx 4\%$). We should stress that the ratio $\Delta P_{Pulse}/P_{Mean}$ can easily be made smaller or larger to maintain a virtually linear relaxation. As a result of this small modulation, the decay in the mols of H_2 is also virtually linear, and the slope of a straight line fitted to the decay in mols of H_2 gives an accurate measurement of the rate of H_2 disappearance from the headspace. Assuming that the change in mols of H_2 gas is due overwhelmingly to reaction with the DEB-Pd/C getter (a good assumption, as we have verified), each slope provides a *direct* measurement of the reaction rate at a particular time, and hence at a particular conversion of the DEB-Pd/C reactant.

We note that the practical lower limit for a measurable reaction rate is governed by the passive outgassing of the instrument, in particular the Inconel elements of the Baratron manometers. Instrument outgassing contributes ~10^{-13} moles H_2 sec^{-1}, so a reasonable lower limit for the measurable absolute reaction rate is ~10^{-11} moles H_2 sec^{-1}, assuming that we wish to limit the instrument artifact to 1% of the measured rate. For reactions with very low specific (mass-normalized) reaction rates, a large quantity of material can be used such that the absolute reaction rate is sufficiently above the lower limit of the instrument, while the specific reaction rate, of course, remains the same.

The data shown in Fig. 3 relate specifically to the case of neat H_2 reactant gas without the use of a diluent. In this situation only the main reactor vessel, (g) in Fig. 2, is used in conjunction with the 1 torr absolute manometer. However, if a gas such as N_2 or He is used as an inert background/diluent, both the main reactor and the reference vessel are required for rate measurements. Here, both are filled with the same background gas to the same pressure and allowed to equilibrate. Then, the valve between them is closed (valve (s) in Fig. 2), and H_2 is dosed to the main reactor in the same way as discussed above for a pure gas experiment. However, the pressure is now measured using the 1 torr differential manometer ((j) in Fig. 2), which gives the pressure *difference* between the main and reference reactor vessels. Regardless of whether an inert diluent is used, the data look essentially the same as shown in Fig. 3.

The ability to measure the rate directly, without numerical differentiation of conversion (mols gas reacted) vs. time data, and without fitting of an assumed rate law to the data, is one of the main strengths of this method. The direct measurement is possible because of the small magnitude of the AC pressure modulation, and hence small incremental conversion associated with each gas aliquot. When the incremental conversion associated with each aliquot is large, its time dependence is usually non-linear. In this case, determination of the reaction rate requires numerical differentiation of the incremental conversion (mols gas reacted) data, or fitting with a mathematical function followed by differentiation. Conversely, determining the reaction rate using the reactor and method described herein, i.e., a least-squares linear fit to mols vs. time data between adjacent local maxima and minima, does not require any assumptions on the part of the experimenter regarding trends in the data or its smoothness. Furthermore, calculation of the uncertainty in slope is well-established and can be easily propagated forward.[47]

Data Acquisition and Control. All data acquisition and control of H_2 gas dosing is performed by a NI LabView custom virtual instrument ("vi") running on a dedicated Windows 10 PC ((r) in Fig. 2). The thin dotted line in Fig. 2 represents multiple data acquisition signals from the manometers ((i), (j), and (k) in Fig. 2) and thermocouples (symbol Ⓣ in Fig. 2) to the PC via a data acquisition chassis (NI No. cDAQ-9178, not shown in Fig. 2). The data acquisition chassis is populated by a 32-channel voltage input module (NI No. NI-9205, not shown in Fig. 2) for manometer signal input and an 8-channel temperature input module (NI No. NI-9212, not shown in Fig. 2) for the signal inputs of the thermocouples. The wider dashed line in Fig. 2 represents the electrical output control signal to the H_2/D_2 doser valve ((f) in Fig. 2) via a 0-1000 V power supply (Oxford Applied Research No. PLV-1000, not shown in Fig. 2).

The NI LabView custom vi has two modes of operation: (i) reaction rate measurement mode, for automated control of H_2 dosing as previously described, and (ii) manual control mode, for use when monitoring the system without computer control of the H_2 doser valve, such as when outgassing the sample, baking the reactor, or monitoring for leaks. For the manual control mode, the user can input/control the following parameters: (i) differential or absolute manometer selection to monitor pressure in case of diluent use or no diluent use, respectively; (ii) data sampling rate, typically 20 Hz, defined as the frequency with which pressure and temperature measurements are taken; and (iii) the number of pressure and temperature samples to average before recording a data point (typically 2-60 points). For the reaction rate mode, in addition to these parameters the user specifies (iv) the target mean H_2 partial pressure P_{Mean}; (v) ½ΔP_{Pulse} (typically $\Delta P_{Pulse}/P_{Mean} \approx 4\%$); and (vi) voltage setpoint specification for the H_2 doser valve (0-1000 V).

The temperature of the system is specified via the embedded controls of the Friocell incubator which can operate at $0 \leq T \leq 100$°C, with a precision of ± 0.05°C as we have verified from independent measurements. The Friocell incubator is not controlled by the LabView vi. The Friocell is allowed to equilibrate for a significant period of time (typically overnight or longer) to allow all contents of the Friocell to arrive at the appropriate temperature before initiating reaction rate measurements.

In the case of experiments using a background gas, charging the reactor and reference with an inert diluent gas is accomplished manually via UHV precision leak valves ((d) in Fig. 2) while monitoring the system pressure on-screen in real time while the vi is running in manual control mode. Once accomplished, the vi is set to reaction rate measurement mode for automated pressure measurement and H_2 reactant gas dosing. The algorithm for automated reaction rate measurement is described in the previous section with reference to Fig. 3.

III. Automated Data Analysis

In a typical reaction experiment, hundreds or thousands of pressure pulse/relaxation cycles may be required to achieve the desired conversion. As such, determination of the reaction rate associated with each pressure decay is best accomplished via an automated data analysis. For this we have developed a custom package of Matlab scripts to analyze the data from the raw data output file (.tdms extension) created by LabView and described in the previous section.[48, 49] In the following paragraphs we describe our Matlab package in some detail. Before proceeding however, we should note that we have also developed a manual analysis routine within OriginLab® OriginPro® software through straightforward implementation of native X-Functions. Although more labor-intensive than the Matlab analysis, this manual analysis gives identical results.

It is important to note that while the instrument produces precise and reproducible data sets that are internally consistent, separate experiments performed under different conditions, such as mean H_2 pressure, diluent gas choice and pressure, reaction temperature, time required to approach full conversion, and so forth, will result in significant variation between data sets. Accordingly, the Matlab package must be versatile such that it can process data acquired from experiments performed under a variety of different conditions.

At its core, our automated Matlab data analysis script package consists of a peak finding solver run inside of a MultiStart object that solves for the number of peaks and their locations by optimizing two variables: threshold and selectivity. Figure 4 illustrates the definitions of threshold and selectivity. Threshold describes the values which the pressure must be greater than to be considered as possible maxima, or less than to be considered as possible minima.[49] Selectivity describes the height above (maxima) or below (minima) the adjacent ordinate data points for a peak to exist.[49]

The goal of the peak finding solver is to minimize the absolute value of the difference between the number of local maximum and minimum peaks. This is expressed mathematically as

$$F_{Obj} = min|(No.of \max peaks) - (No.of \min peaks)| \leq 1 \tag{2}$$

The automated data analysis package achieves this by finding the number of local maxima in a particular data set, subsequently and separately finding the number of local minima, and then comparing the two values to see if Eq. (2) is satisfied. This analysis occurs by iteratively optimizing for threshold and selectivity within a set of mathematical constraints set by the user at the beginning of the analysis. The MultiStart optimization repeats this sequence for a user-determined number of iterations (typically 10-1000 iterations) using randomly generated initial conditions in an attempt to find a global solution within the given constraints. The .tdms file reader and the core peak finding scripts described above are third-party scripts that can be retrieved from the Matlab Central File Exchange.[48, 49]

As mentioned above, the automated analysis iteratively optimizes threshold and selectivity parameters within given boundary constraints to satisfy Eq. (2). It is important to note that the high precision and repeatability of the raw data obtained by the instrument is the primary factor that allows for automation of the data analysis. To illustrate this, consider the ordinate values of the local maxima and minima in Fig. 3(c). These maxima and minima are extremely consistent, having a relative uncertainty of ±0.15%. If the local maxima and minima values showed substantial variability, the boundary conditions and set of randomly generated initial conditions would require significant expansion. It is possible the user would be able to compensate by increasing the number of iterations, however, it is more likely that a reasonable solution would be unattainable or reaching a solution may require a different optimization algorithm altogether.

Once the number and location of the local maxima and minima have been determined, the decay in moles of H_2 gas between adjacent local maximum-minimum pairs is fitted with a straight line via a least-squares regression. Figure 3(d) illustrates the slopes of the lines fitted to the data between a few local maximum-minimum pairs. The slope represents a direct measurement of the reaction rate. The results of these fits are shown in Fig. 5, which plots the specific reaction rate (i.e., normalized by the sample mass) versus time. Figure 6 shows the same data as Fig. 5, but plotted as (a) fractional conversion vs. time, and (b) specific reaction rate vs. fractional conversion. Note that the fractional conversion is easily computed via integration of the rate vs. time data in Fig. 5.

We should point out that the data in Fig. 5 and Fig. 6 highlight a key attribute of our semi-batch reactors: the ability to resolve detailed features of the reaction kinetics that is possible when rates are measured directly, but in our experience may be difficult when conversion (accumulated signal) vs. time is measured and then differentiated or otherwise analyzed. As an example, notice the shoulder in the Fig. 5 data at ≈ 1 day. This may represent a change in the reaction mechanism or another nuance of the chemistry at work. Similar features can be observed in Fig. 6(b) as well. The origin of these features is currently under investigation.

IV. Evaluation of Reactor Performance

Figure 7 and Fig. 8 compare reaction rate and conversion data for several lots of DEB-Pd/C getter pellets manufactured at the Honeywell Kansas City National Security Complex. Here we include our data for lots X101, X201, and X301, measured using the semi-batch apparatus described herein, as well as literature data from Powell.[20, 50, 51] Lot information is not reported for the Powell data. All experiments were conducted using nominally identical pellets (but from different lots) at 750 mtorr neat H_2 (no diluent) and room temperature (25°C for X101 – X301, and 21°C for Powell). The Powell data were measured using a gas buret system that functions similarly to a Sieverts' apparatus.[52, 53] In those experiments, rates were derived from single pressure pulses that were allowed to decay from ~750 mtorr to <1 mtorr. The result was a nonlinear pressure vs. time trace that was analyzed with an empirical kinetic model to determine reaction rates.[20, 50, 51]

The lot-to-lot variability seen in our X101 – X301 data indicates that comparison of absolute H_2 reaction rates measured using different techniques, i.e., the Powell gas buret method vs. our semi-batch method, is meaningful to assess reactor performance *only* when identical material lots can be measured. Most likely, the variability between nominally identical but different getter lots is associated with poorly- or un- controlled aspects of the manufacturing process. Indeed, some lot-to-lot variability of properties is to be expected for composite materials whose processing flowsheet is complex.

In view of this variability, we attempted to identify a "standard" material in the literature whose reaction kinetics with H_2, O_2, or other gas are well-known and reproducible. However, in contrast to measurements in other fields of science where accurate standards are well-established, for example the lattice parameter of Si or LaB_6, or the thermal expansion coefficient of well-annealed OFHC Cu, we were unable to identify a standard that is both reproducible and relevant to the experimental pressure and temperature capabilities of our reactors. Therefore, to assess the performance of our semi-batch reactors we have examined the precision and reproducibility of our data. As demonstrated in Fig. 5 - Fig. 8, the rates determined using the semi-batch reactors have high precision, with little scatter and small uncertainty. A typical relative uncertainty is $< \pm 0.05\%$, and the error bars associated with each data point are far smaller than the point itself. This contrasts with the Powell data in Fig. 7 and Fig. 8, where the large scatter implies a significantly larger uncertainty.

Figure 9 shows the specific reaction rate as a function of time, the time dependence of the fractional conversion, and the specific reaction rate as a function of conversion in panels (a), (b), and (c), respectively, for replicate measurements that we have performed on lot X101 of the DEB-Pd/C pellets. Experiments were performed on four separate occasions over a time span greater than three years, using two different semi-batch reactor systems. (We have constructed four such reactors.) Clearly, the data are highly reproducible among materials of the same pedigree, again pointing to the performance of the semi-batch reactors. We should mention that at least some of the small variations observed between measurements might be attributable to pellet-to-pellet variability within a given material lot, possibly due to inhomogeneities resulting from imperfect blending operations.

In closing this section we should add that other researchers have investigated the kinetics DEB-Pd/C hydrogen scavengers but their experimental parameters such as temperature, pressure, and material composition are inconsistent with the present work and hence their kinetic data cannot be compared to our data and the data of Powell.[13, 16, 17, 21, 44, 54]

V. Conclusion

We have described the design, construction, and operation of a semi-batch reactor system for the measurement of gas-sold reaction kinetics at pressures ranging from 1 mtorr to 1500 torr. This manometric-based measurement system has proven to be especially useful in cases where the volatility of solid reactants or products limits the efficacy of thermogravimetric methods. For the purpose of measuring gas-solid reaction rates, the reactor and methodology described here provide an advantage compared to the often-used Sieverts' technique. Specifically, the Sieverts' method has the drawback of allowing a large relative pressure decay to occur between gas pulses. Our semi-batch approach improves upon the Sieverts' method by limiting the pressure decay to a small percentage of the initial pressure before more reactant gas is dosed into the semi-batch reactor. This methodology facilitates direct measurement of the reaction rate via linear fits to the pressure relaxation (decay) data. We have found that this superposition of a small AC pressure perturbation on a DC pressure background yields rate data of high precision and reproducibility, thus allowing even small features in reaction rate and conversion curves to be measured.

We have also demonstrated instrument performance through measurements of the hydrogenation kinetics of 1,4-bis(phenylethynyl)benzene (DEB)-Pd/C H_2 getters. The instrument shows good reproducibility during repeated measurements performed on nominally identical DEB getter material. We do observe significant variations in rate between different getter lots, as might be expected for a composite material with a complex processing flowsheet. Comparison of our DEB hydrogenation data with literature data from Powell, collected using a gas buret method, indicates that our semi-batch method yields rate data of substantially higher precision.

While the manometric, semi-batch method does lend itself to niche chemical systems such as the low-temperature, subatmospheric catalytic hydrogenation of DEB discussed here, it can also be modified for other chemical systems and reaction conditions. All system components may be exchanged for others which tolerate more severe temperature and pressure ranges. Additionally, adding a gas chromatograph, mass spectrometer, binary gas analyzer, or a tunable diode laser, and integrating such gas composition measurements with doser valve operation, can facilitate application of this design to systems having more complex gas matrices.

Acknowledgements

This work was supported by the US Department of Energy through the Los Alamos National Laboratory. Los Alamos National Laboratory (LANL) is operated by Triad National Security, LLC, for the National Nuclear Security Administration of U.S. Department of Energy (Contract No. 89233218CNA000001). Financial support for this work was provided by the Aging and Lifetimes Program and the B61 Life Extension Program at LANL.

Data Availability Statement

The data that support the findings of this study are available from the corresponding author upon reasonable request.

References

[1]S. Vyazovkin, A. K. Burnham, J. M. Criado, L. A. Pérez-Maqueda, C. Popescu and N. Sbirrazzuoli, Thermochimica Acta **520** (1-2), 1-19 (2011).

[2]H. S. Fogler, *Elements of Chemical Reaction Engineering*, 4 ed. (Pearson, Upper Saddle River, NJ, 2006).

[3]O. Levenspiel, *Chemical Reaction Engineering*, 3 ed. (Wiley, New York, 1999).

[4]J. Szekely, J. W. Evans and H. Y. Sohn, *Gas-Solid Reactions*. (Academic Press, New York, 1976).

[5]J. P. Stanford, M. C. Soto, P. H. Pfromm and M. E. Rezac, Catalysis Today **268**, 19-28 (2016).

[6]X. L. Wang and S. Suda, International Journal of Hydrogen Energy **15** (8), 569-577 (1990).

[7]See https://www.tainstruments.com/products/thermal-analysis/ for a list of commercially available thermal analysis instruments.

[8]See https://www.perkinelmer.com/category/thermal-analysis-instruments for a list of commercially available thermal analysis instruments.

[9]See https://www.ssi.shimadzu.com/products/thermal-analysis/index.html for a list of commercially available thermal analysis instruments.

[10]S. Vyazovkin, K. Chrissafis, M. L. Di Lorenzo, N. Koga, M. Pijolat, B. Roduit, N. Sbirrazzuoli and J. J. Suñol, Thermochimica Acta **590**, 1-23 (2014).

[11]R. L. Courtney and L. A. Harrah, Journal of Materials Science **12** (1), 175-186 (1977).

[12]R. E. Trujillo and R. L. Courtney, Journal of Materials Science **12** (5), 937-945 (1977).

[13]L. N. Dinh, M. A. Schildbach, J. L. Herberg, A. P. Saab, J. C. Weigle, S. C. Chinn, R. S. Maxwell and W. McLean, J. Nucl. Mater. **382** (1), 51-63 (2008).

[14]A. Maiti, L. N. Dinh, T. F. Baumann, R. S. Maxwell and A. P. Saab, Chemical Physics Letters **475** (4), 223-226 (2009).

[15]G. L. Powell, Journal of Alloys and Compounds **446-447**, 402-404 (2007).

[16]M. Balooch, W. E. Wang and J. R. Kirkpatrick, J. Polym. Sci. Pt. B-Polym. Phys. **39** (4), 425-431 (2001).

[17]L. N. Dinh, G. A. Cairns, R. Krueger, B. P. Mayer and R. S. Maxwell, J. Nucl. Mater. **442** (1-3), 298-305 (2013).

[18]S. Yamanaka, Y. Sato, H. Ogawa, Y. Shirasu and M. Miyake, J. Nucl. Mater. **179**, 303-307 (1991).

[19]J. B. Conn, G. B. Kistiakowsky and E. A. Smith, J. Am. Chem. Soc. (61), 1868-1876 (1939).

[20]G. L. Powell, Report No. Y/DZ-2279/R1, Y-12 National Security Complex, Oak Ridge, TN, 2002.

[21]M. Balooch, W. E. Wang and J. D. LeMay, J. Nucl. Mater. **270** (1-2), 248-252 (1999).

[22]H. N. Sharma, E. A. Sangalang, C. K. Saw, G. A. Cairns, W. McLean, R. S. Maxwell and L. N. Dinh, Journal of Chemical Physics **147** (19), 9 (2017).

[23]P. A. Giguere and I. D. Liu, Report No. OSR-TN-55-383; AD-83048, Laval Univ., Quebec, 1955.

[24]G. R. Thomas and N. N. Lichtin, Rev. Sci. Instrum. **24** (8), 661-664 (1953).

[25]R. Vestin, I. Cedergren and L. Arro, Acta Chem. Scand. **17** (4), 1093-& (1963).

[26]D. P. Broom, C. J. Webb, K. E. Hurst, P. A. Parilla, T. Gennett, C. M. Brown, R. Zacharia, E. Tylianakis, E. Klontzas, G. E. Froudakis, T. A. Steriotis, P. N. Trikalitis, D. L. Anton, B. Hardy, D. Tamburello, C. Corgnale, B. A. van Hassel, D. Cossement, R. Chahine and M. Hirscher, Appl. Phys. A-Mater. Sci. Process. **122** (3), 21 (2016).

[27]A. Anani, A. Visintin, K. Petrov, S. Srinivasan, J. J. Reilly, J. R. Johnson, R. B. Schwarz and P. B. Desch, Journal of Power Sources **47** (3), 261-275 (1994).

[28]H. T. Bach, R. B. Schwarz and D. G. Tuggle, Fusion Science and Technology **48** (1), 545-550 (2005).

[29]H. T. Bach, T. J. Venhaus, S. N. Paglieri, H. Oona, T. H. Allen, R. B. Schwarz and J. R. Wermer, Journal of Alloys and Compounds **446-447**, 567-570 (2007).

[30]R. B. Schwarz, A. K. Khachaturyan, A. Caro, M. I. Baskes and E. Martinez, Journal of Materials Science **55** (11), 4864-4882 (2020).

[31]V. Sinha, R. B. Schwarz, M. J. Mills and J. C. Williams, Scripta Materialia **153**, 81-85 (2018).

[32]V. Sinha, R. B. Schwarz, M. J. Mills and J. C. Williams, Acta Materialia **188**, 315-327 (2020).

[33]See http://www.quantachrome.com/gassorption/autosorb_iq.html for a description of a commercially abailable Sieverts instrument.

[34]See https://www.micromeritics.com/Product-Showcase/3Flex-Surface-Characterization-Analyzer1.aspx for a description of a commercially abailable Sieverts instrument.

[35]S. Lowell, J. E. Shields, M. A. Thomas and M. Thommes, *Characterization of Porous Solids and Powders: Surface Area, Pore Size and Density*. (Springer, Dordrecht, 2006).

[36]D. P. Broom, *Hydrogen Storage Materials : The Characterisation of Their Storage Properties*. (Springer, London, UK, 2011).

[37]F. Rouquerol, J. Rouquerol, K. S. W. Sing, P. L. Llewellyn and G. Maurin, *Adsorption by Powders and Porous Solids: Principles, Methodology and Applications*, Second edition. ed. (Academic Press, Oxford, 2014).

[38]M. Bielmann, S. Kato, P. Mauron, A. Borgschulte and A. Züttel, Rev. Sci. Instrum. **80** (8), 083901 (2009).

[39]A. Policicchio, E. Maccallini, G. N. Kalantzopoulos, U. Cataldi, S. Abate, G. Desiderio and R. G. Agostino, Rev. Sci. Instrum. **84** (10), 10 (2013).

[40]N. S. Anand, S. Pati, R. A. Jat, S. C. Parida and S. K. Mukerjee, International Journal of Hydrogen Energy **40** (1), 444-450 (2015).

[41]M. Balcerzak, J. Jakubowicz, T. Kachlicki and M. Jurczyk, Journal of Power Sources **280**, 435-445 (2015).

[42]R. A. Jat, S. C. Parida, J. Nuwad, R. Agarwal and S. G. Kulkarni, Journal of Thermal Analysis and Calorimetry **112** (1), 37-43 (2013).

[43]J. Li, P. Fan, Z. Z. Fang and C. Zhou, International Journal of Hydrogen Energy **39** (14), 7373-7381 (2014).

[44]L. N. Dinh, A. G. Cairns, R. A. Strickalnd, W. McLean and R. S. Maxwell, J. Phys. Chem. A **119**, 8 (2015).

[45]LabView 2019, National Instruments, https://www.ni.com/en-us.

[46]MATLAB, The Mathworks, Inc., https://www.mathworks.com/.

[47]J. R. Taylor, *An Introduction to Error Analysis: The Study of Uncertainties in Physical Measurements*, 2 ed. (University Science Books, Sausalito, CA, 1997).

[48]J. Hokanson, TDMS Reader, MATLAB Central File Exchange, https://www.mathworks.com/matlabcentral/fileexchange/30023-tdms-reader (March 5, 2020).

[49]N. Yoder, peakfinder, MATLAB Central File Exchange, https://www.mathworks.com/matlabcentral/fileexchange/25500-peakfinder-x0-sel-thresh-extrema-includeendpoints-interpolate (March 5, 2020).

[50]G. L. Powell, *Reaction of hydrogen with an organic hydrogen getter*. (The Minerals, Metals, & Materials Society, 2004).

[51]G. L. Powell, *The hydriding kinetics of organic hydrogen getters*. (The Minerals, Metals & Materials Society, 2004).

[52]G. L. Powell, Zeitschrift Fur Physikalische Chemie Neue Folge **164**, 1227-1232 (1989).

[53]G. L. Powell, W. L. Harper and J. R. Kirkpatrick, Journal of the Less-Common Metals **172**, 116-123 (1991).

[54]E. A. Sangalang, H. N. Sharma, C. K. Saw, R. Gollott, S. M. Matt, T. S. Wilson, W. McLean, R. S. Maxwell and L. N. Dinh, ACS Appl. Mater. Interfaces **12** (3), 3993-4001 (2020).

Figures

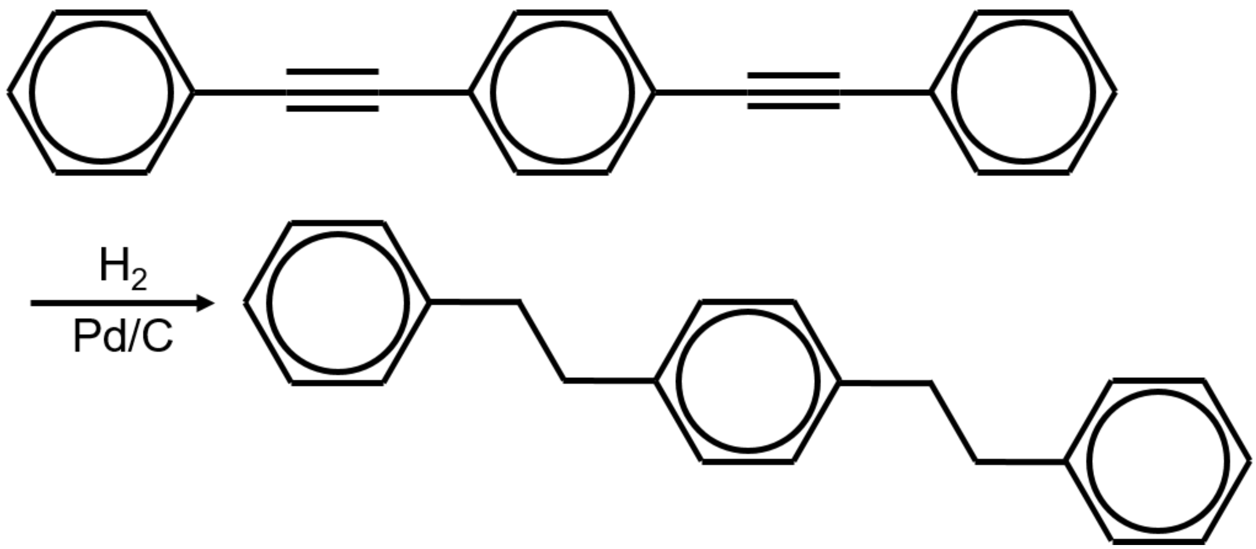

FIG. 1. Catalytic hydrogenation of 1,4-bis(phenylethynyl)benzene (DEB). Chemical intermediates in the reaction network are not shown.

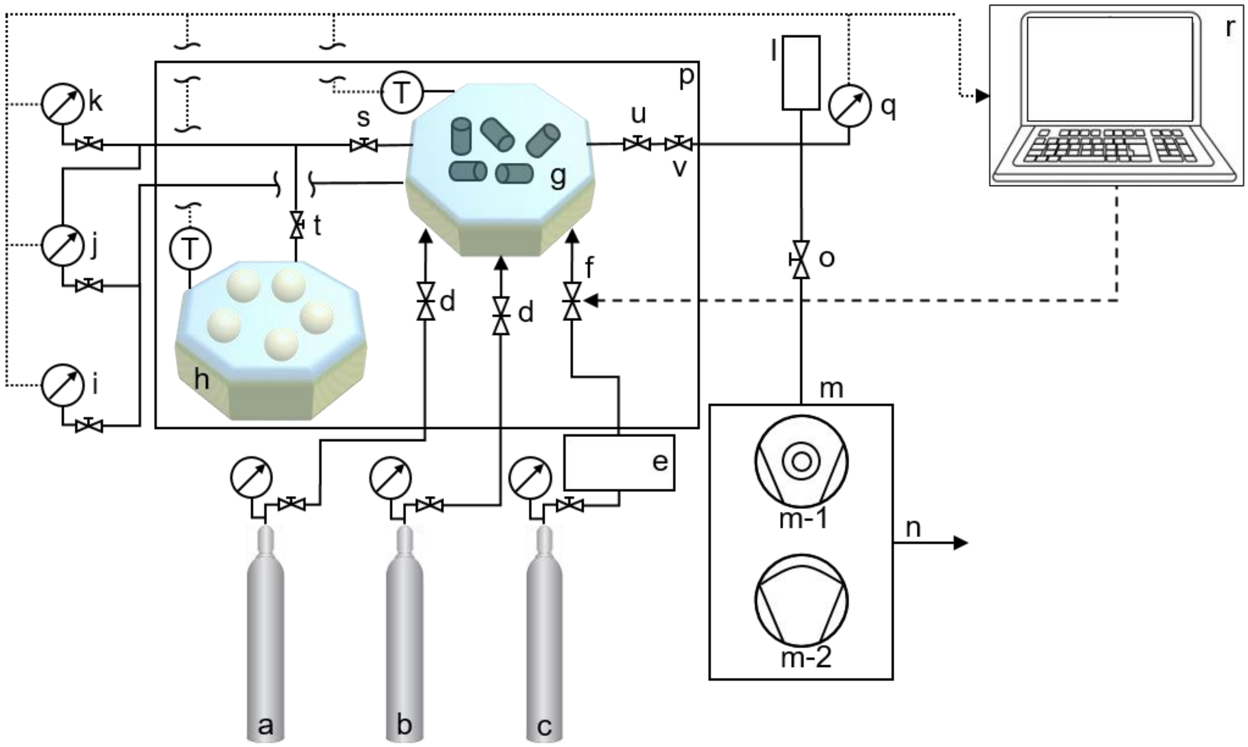

FIG. 2. Schematic of gas-solid reactor system. (a) He diluent gas cylinder; (b) N_2 purge /diluent gas cylinder; (c) H_2 reactant gas cylinder; (d) ultra-high-vacuum, manually controlled precision leak valves; (e) hydrogen purifier; (f) ultra-high-vacuum, piezoelectrically controlled, leak/doser valve; (g) gold-plated main reactor vessel containing DEB H_2 getter pellets; (h) gold-plated reference vessel (virtually identical to main reactor) containing 13x sieves and/or other gas scavengers to prevent pressure build-up; (i) 1 torr absolute pressure manometer; (j) 1 torr differential pressure manometer; (k) 1000 torr absolute pressure manometer; (l) mass spectrometer; (m) vacuum pumping station containing (m-1) turbo vacuum pump, (m-2) dry diaphragm backing pump; (n) vent to fume hood; (o) gate valve; (p) envelope of Friocell incubator; (q) compact full-range pressure gauge (10^{-9} torr $\leq P \leq$ 1000 torr); (r) dedicated Windows 10 PC running a custom NI LabView vi which uses temperatures and pressures to dose H_2/D_2 via valve (f); (s) and (t) all-metal bellows-sealed valves separating reference from reactor vessels; (u) and (v) all-metal bellows-sealed valves separating reactor system from vacuum system. Note that all unlabeled valves in this schematic are also all-metal and bellows-sealed. The symbol Ⓣ represents 2 thermocouples attached to either the reactor (g) or reference (h) volumes. The thin dotted line represents electrical data acquisition signals from the manometers and thermocouples. The wider dashed line represents an electrical output control signal to the H_2/D_2 leak valve (f).

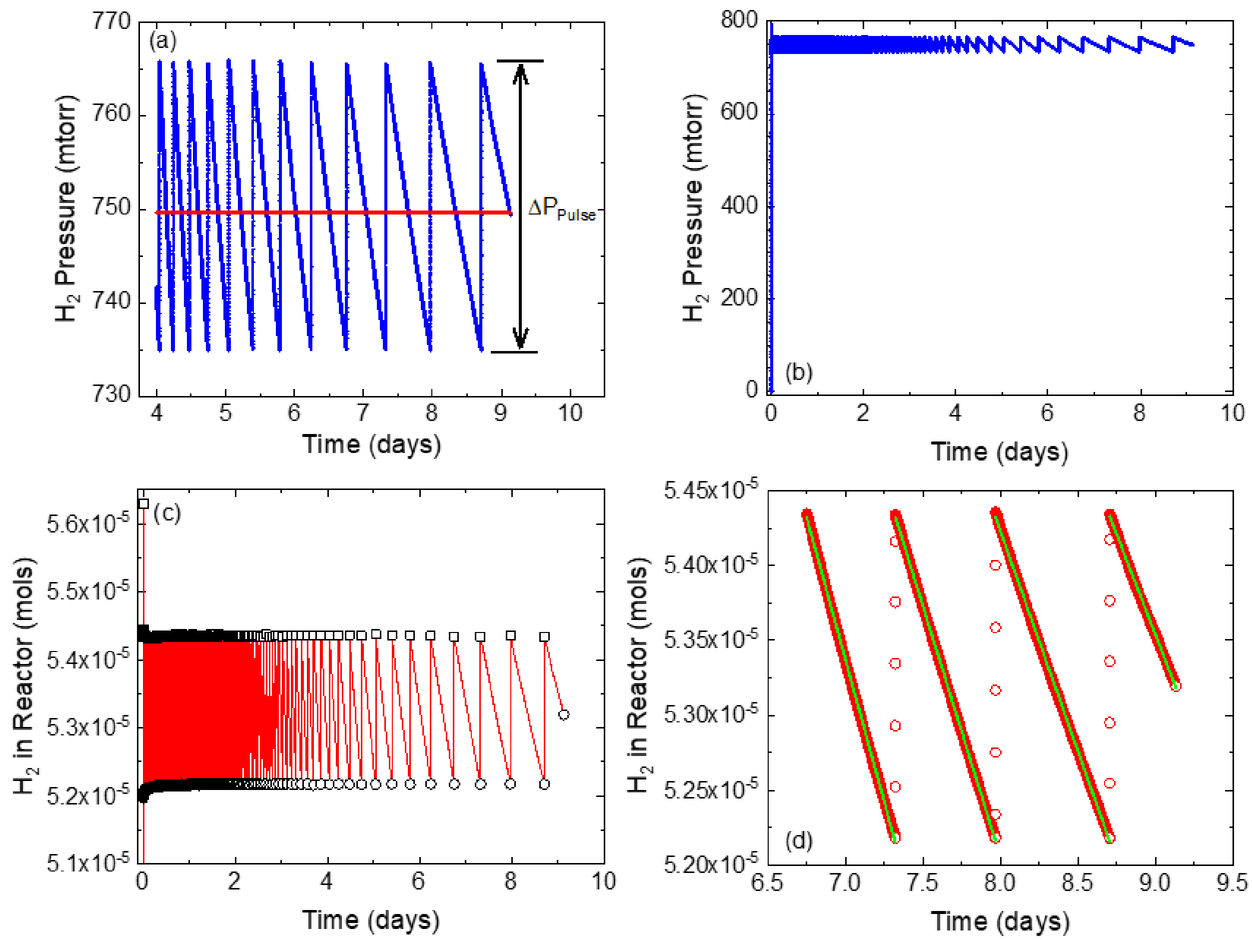

FIG. 3. Time dependence of the absolute pressure and moles of H_2, measured during a typical experiment involving reaction of neat H_2 (no background gas) with DEB-Pd/C. Here, the nominal mean pressure is P_{Mean} = 750 mtorr, and ½ΔP_{Pulse} = 15 mtorr. Panel (a) shows several pressure decay/relaxation cycles denoting P_{Mean} (red horizontal line) and ΔP_{Pulse} (black span). Panel (b) shows the raw pressure data for the entire experiment, collected using our custom LabView virtual instrument (vi). Panel (c) shows the moles of H_2 in the reactor, as computed from the pressure data in panel (b) using the ideal gas law. Here the maxima and minima are denoted by black squares and circles respectively. Panel (d) shows a magnified view of mols H_2 vs. time for 4 relaxation cycles (red circles), where the slopes of the H_2 decays are fit with straight lines (green). The last relaxation cycle shown, at about 9 days, was the final cycle of this particular experiment.

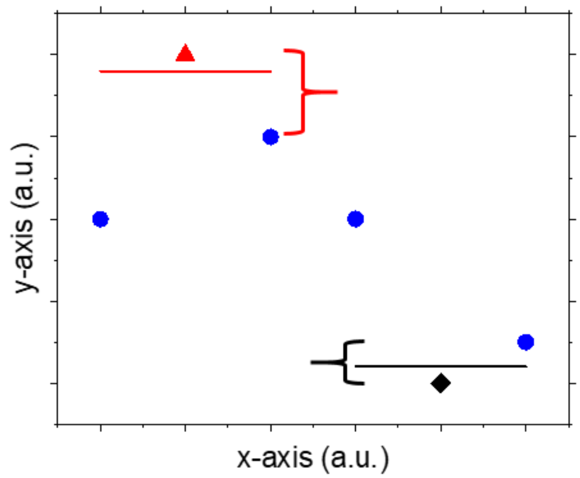

FIG. 4. Illustration of threshold and selectivity. Blue circles represent arbitrary data. The red triangle and black diamond represent the local maximum and minimum respectively. Maximum and minimum thresholds are shown as red and black horizontal lines, respectively. Selectivities for the maximum and minimum are shown as red and black brackets, respectively.

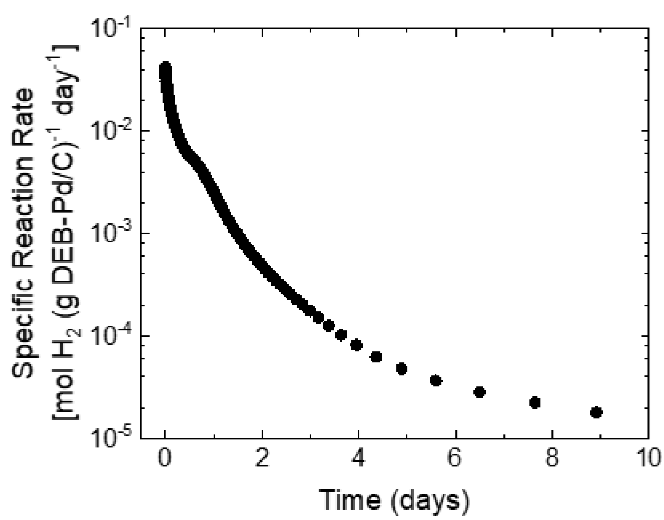

FIG. 5. Time dependence of the specific (mass-normalized) reaction rate, as determined by straight line fits to the pressure decay data between the local maxima and minima shown in Fig. 3(d).

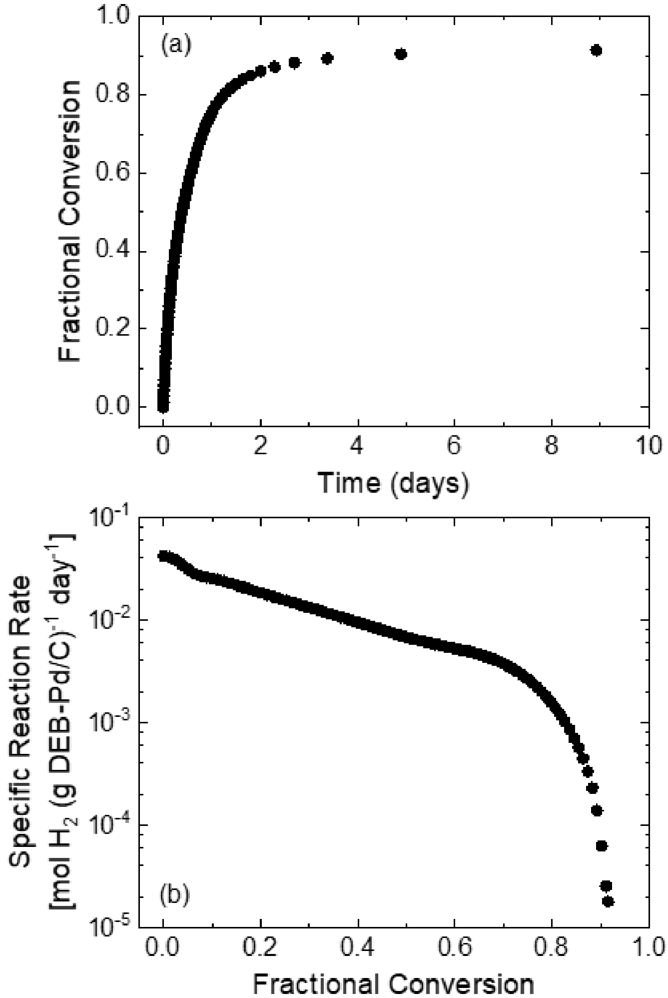

FIG. 6. Alternative presentations of data shown in Fig. 5: (a) Fractional conversion as a function of time, (b) Specific (mass-normalized) reaction rate as a function of fractional conversion. Conversion is easily calculated via integration of the reaction rate data in Fig. 5.

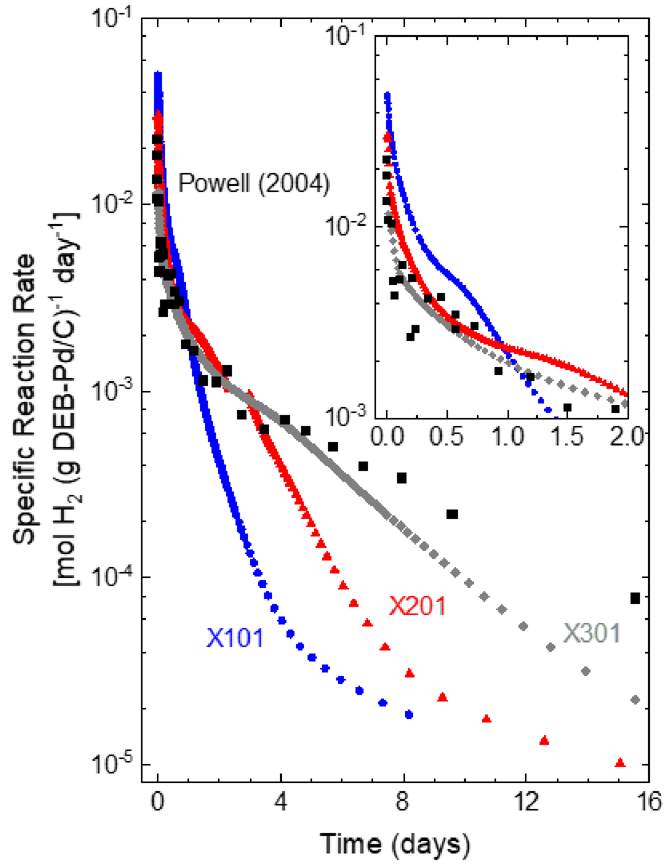

FIG. 7. Comparison of the time dependence of the specific (mass-normalized) reaction rates for several lots of DEB-Pd/C getter pellets, measured by the authors, together with literature data from Powell.[50, 51] The inset shows a magnification of the 0-2 day time scale. Experiments were conducted using 750 mtorr neat H_2, without use of a diluent, at 25°C for X101-X301 lots, and at 21°C for Powell data. Lot X101 is shown by blue circles, X201 by red triangles, X301 by gray diamonds, and Powell data by black squares. The pedigree (lot) of Powell's DEB-Pd/C getter pellets is unknown to the authors.

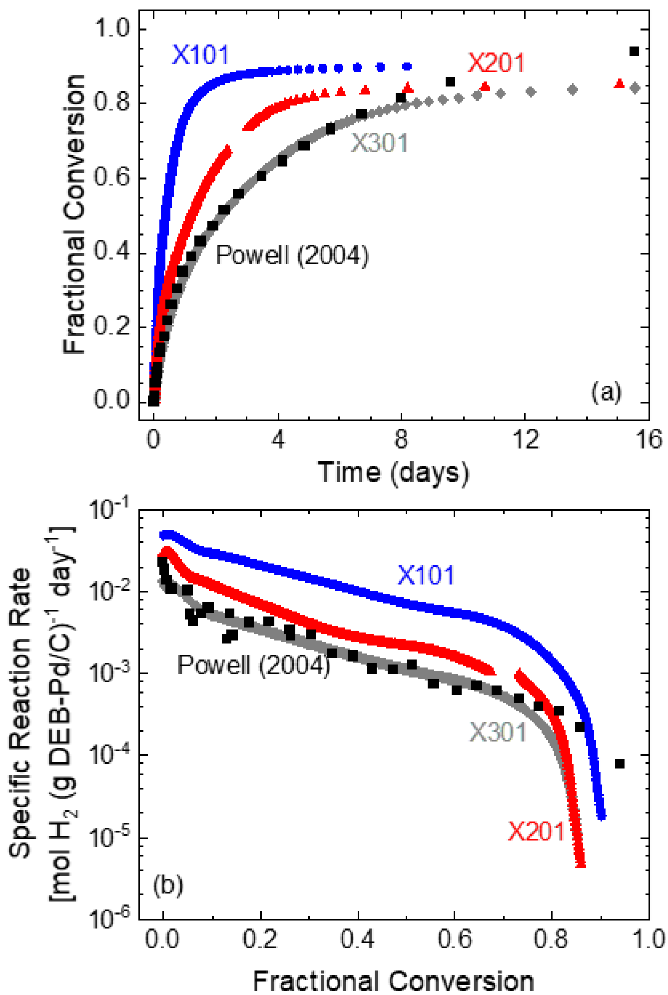

FIG. 8. Further comparison of reaction rate and conversion data for several lots of DEB-Pd/C getter pellets, measured by the authors, and literature data from Powell.[50, 51] This figure is an alternative presentation of the lot comparison shown in Fig. 7: Panel (a) Fractional conversion as a function of time, (b) Specific (mass-normalized) reaction rate as a function of fractional conversion. Experiments were conducted using 750 mtorr H_2 without a diluent gas at 25°C for lots X101-X103 and at 21°C for data from Powell. Lot X101 is shown by blue circles, X201 by red triangles, X301 by gray diamonds, and Powell data by black squares. Data for lots X101-X301 represent experiments performed by the authors. The pedigree (lot) of Powell's DEB-Pd/C getter pellets is unknown to the authors.

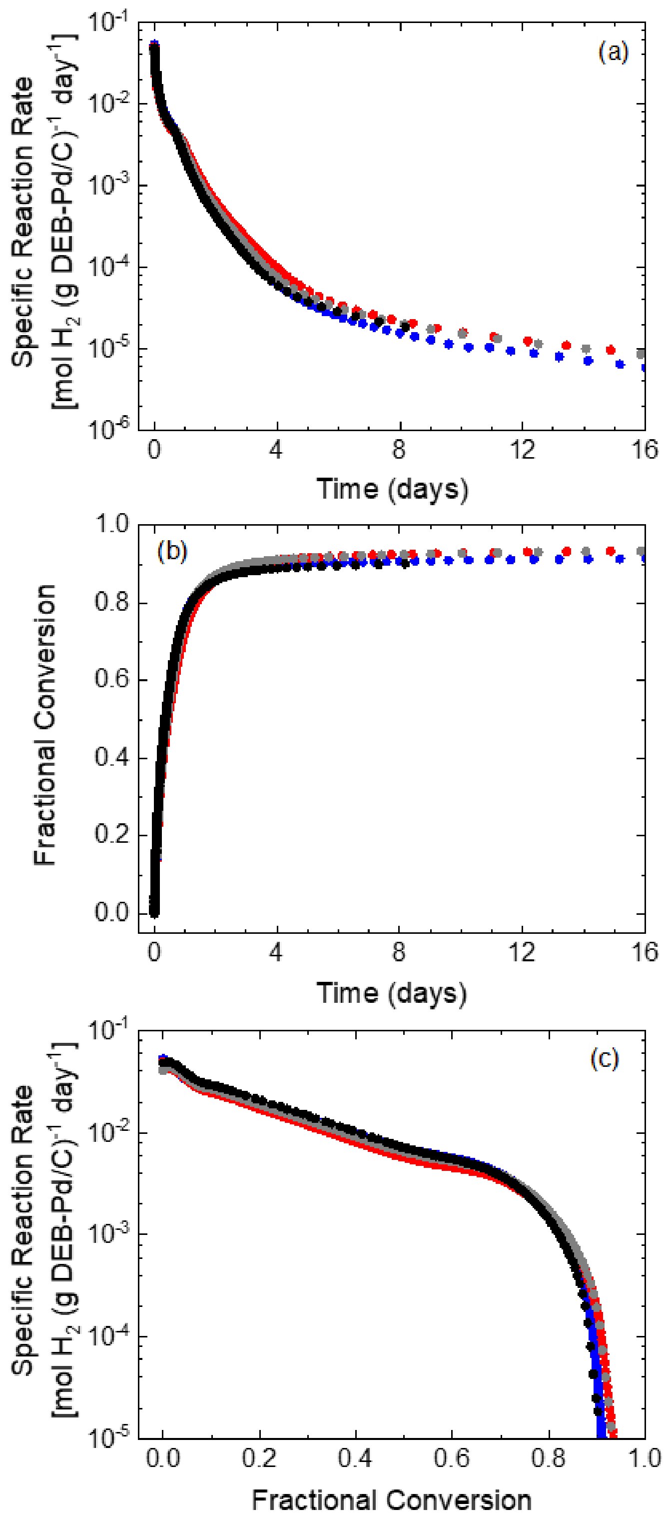

FIG. 9. Comparison of four separate rate-measurement experiments performed on material lot X101 under the same conditions: 25°C and H_2 pressure of 750 mtorr. Red, gray and black circles represent experiments performed on Reactor 1 beginning on 06/22/2015, 07/23/2015, and 08/20/2018, respectively. Blue circles represent an experiment performed on Reactor 2

beginning on 12/22/2018. Panel (a) shows the specific (mass-normalized) reaction rate as a function of time, (b) the fractional conversion as a function of time, and (c) the specific reaction rate as a function of conversion. No diluent gas was used.